

**Cite this article as:** Yang Yu, Chen Junyu, Ma Tongxiang, et al. Mechanical Properties and Corrosion Resistance Behavior of CoCrFeNi High-Entropy Alloy Prepared by Mechanical Alloying Coupled with Vacuum Hot Pressing Sintering[J]. Rare Metal Materials and Engineering, 2022, 51(09): 3182-3188.

ARTICLE

# Mechanical Properties and Corrosion Resistance Behavior of CoCrFeNi High-Entropy Alloy Prepared by Mechanical Alloying Coupled with Vacuum Hot Pressing Sintering

Yang Yu<sup>1,2</sup>, Chen Junyu<sup>1,2</sup>, Ma Tongxiang<sup>1,2</sup>, Hu Meilong<sup>1,2</sup>

<sup>1</sup> College of Materials Science and Engineering, Chongqing University, Chongqing 400044, China; <sup>2</sup> Chongqing Key Laboratory of Vanadium-Titanium Metallurgy and New Materials, Chongqing University, Chongqing 400044, China

**Abstract:** CoCrFeNi high-entropy alloy (HEA) was fabricated by mechanical alloying (MA) and vacuum hot pressing sintering (VHPS). The phase and microstructure of alloys were characterized by X-ray diffraction, scanning electron microscope, inductively coupled plasma-optical emission spectrometer, and optical microscope. The mechanical properties and corrosion resistance were investigated by universal tensile machine, Vickers hardness tester, and electrochemical workstation. Results show that CoCrFeNi HEA prepared by MA-VHPS exhibits excellent ultimate tensile strength and elongation, compared with those prepared by the arc-melting method and the combined method of the electrochemical reduction (FFC) with VHPS. The hardness of CoCrFeNi HEA prepared by MA-VHPS is twice larger than that prepared by arc-melting. The CoCrFeNi HEA prepared by MA-VHPS displays the corrosion resistance in 0.5 mol/L H<sub>2</sub>SO<sub>4</sub>, 1 mol/L KOH, and 3.5wt% NaCl solutions comparable to that of the 304 stainless steel and CoCrFeNi HEAs prepared by FFC-VHPS or arc-melting.

**Key words:** high-entropy alloy; mechanical alloying; vacuum hot pressing sintering; mechanical property; corrosion resistance

High entropy alloys (HEAs), namely the multi-principal-element alloys<sup>[1,2]</sup>, are solid solutions of equiatomic or near-equiatomic (5at%~35at%) composition with several principal elements, such as Fe, Al, Mg, Ti, and Cu. The high configurational entropy of the multi-component alloys can induce serious lattice distortion and sluggish diffusion. The four core effects, including the high entropy effect, sluggish diffusion effect, lattice distortion effect, and cocktail effect, lead to the formation of simple solid-solutions or amorphous structure of HEAs, rather than the intermetallics. Consequently, HEAs often exhibit high hardness, excellent mechanical properties, and good resistance to wear, oxidation, and corrosion<sup>[3-6]</sup>.

Liquid-phase synthesis methods, such as arc melting<sup>[7-9]</sup>, selective laser melting<sup>[10,11]</sup>, and Bridgman solidification<sup>[12,13]</sup>, are commonly used to prepare HEAs, although they have the disadvantages of high processing temperature and uncertain homogeneity degree of alloys. In addition, obvious element segregation easily occurs during the melt solidification. Due

to the solidification shrinkage and segregation, the properties of the melted alloys cannot meet the requirements. Thus, further forging and heat treatment are required to overcome these problems. Powder metallurgy is one of the solid-phase synthesis methods, and it is convenient for alloy synthesis. Currently, the mechanical alloying (MA) method is widely used for the synthesis of nanocrystalline materials with uniform microstructure. Ref. [14-16] also reported the synthesis of HEAs by MA. Vacuum hot pressing sintering (VHPS) is a simple rapid solid state processing method to synthesize bulk HEAs at low temperatures<sup>[17,18]</sup>. Combined with VHPS method which can mold and sinter the raw material powders simultaneously, the bulk HEAs can be easily prepared by MA. In addition, the low processing temperature of VHPS can effectively prevent the grain growth, thereby significantly improving the mechanical properties of the bulk HEAs due to the fine grain strengthening effect.

In this research, CoCrFeNi equiatomic HEAs were synthesized by MA followed by VHPS. The mechanical

Received date: September 05, 2021

Corresponding author: Hu Meilong, Ph. D., Professor, College of Materials Science and Engineering, Chongqing University, Chongqing 400044, P. R. China, Tel: 0086-23-65112631, E-mail: hml@cqu.edu.cn.

Copyright © 2022, Northwest Institute for Nonferrous Metal Research. Published by Science Press. All rights reserved.

properties of CoCrFeNi HEAs prepared by MA-VHPS were investigated and compared with those prepared by arc-melting method<sup>[7-9,19]</sup> and the combined method of electro-deoxidization of the metal oxides and vacuum hot pressing sintering (FFC-VHPS)<sup>[20]</sup> process. The corrosion behavior of CoCrFeNi HEA prepared by MA-VHPS was studied and compared with that of the 304 stainless steel (304SS) and CoCrFeNi HEA prepared by FFC-VHPS process in 0.5 mol/L H<sub>2</sub>SO<sub>4</sub>, 1 mol/L KOH, and 3.5wt% NaCl aqueous solutions.

## 1 Experiment

High purity metal powders of Co (>99.0wt% ), Cr (>99.99wt% ), Fe (>99.9wt% ), and Ni (>99.9wt% ) with particle size ≤45 μm were used as starting materials. These powders were mixed at equiatomic ratio and milled in a high-energy planetary ball miller (Retch PM100) at 250 r/min for 24 h in the argon atmosphere with the mass ratio of ball:powder=10:1.

The milled CoCrFeNi HEA powders were placed in a graphite mould and then put into the VHPS furnace with the vacuum level of 2 Pa. During VHPS process, the temperature was 1373 K, the heating rate was 10 K/min, the pressure was 30 MPa, and the holding time was 1 h. The hot-pressed HEAs were cut into tensile specimens, and then ground and polished by SiC abrasive paper and cashmere polishing cloth, respectively. The polished tensile specimen is shown in Fig.1.

The phase components of the milled powders and bulk HEA specimen were determined by X-ray diffraction (XRD, D/max 2500PC, Rigaku, Japan). The morphology and chemical composition of the milled powders and bulk HEA specimen were characterized by scanning electron microscope (SEM) and energy dispersive X-ray spectroscopy (EDS, TESCAN VEGA II with Oxford INCA Energy 350).

The composition of HEA powder after MA was determined by inductively coupled plasma-optical emission spectrometer (ICP-OES, ICAP6300 DUO, ThermoFisher Scientific). The metallographic characteristics were analyzed by optical microscope (OM, CX40M, SUNNY, China). Aqua regia was used as the metallographic corrosion solution. The fractural cross-section morphologies of the bulk HEA specimens were characterized by SEM. The oxygen content of HEAs was analyzed by the oxygen nitrogen hydrogen analyzer (THC600, Germany). The mechanical properties were measured through tensile tests with an initial strain rate of  $1.0 \times 10^{-4} \text{ s}^{-1}$ . The hardness of HEAs was measured by the Vickers hardness tester (Model HV-115, Mitutoyo, Kanagawa, Japan) under the

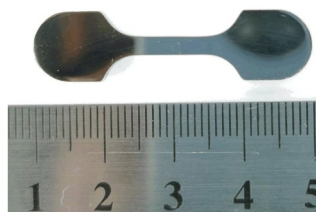


Fig.1 Appearance of polished tensile specimen of CoCrFeNi HEA

load of 100 g and the holding time of 10 s. The corrosion test was conducted on an electrochemical workstation (CHI 660, Shanghai Chenhua Instrument Co., Ltd, China). The working electrode, reference electrode, and counter electrode were the HEA specimen, commercial Ag/AgCl electrode, and a platinum sheet, respectively. The potential scan rate was 2 mV/s.

## 2 Results and Discussion

### 2.1 Structure and morphology characterizations

Fig.2 presents XRD pattern of the CoCrFeNi HEA powder prepared by MA. The results show that the single face-centered cubic (fcc) phase with (111), (200), and (220) planes can be observed after MA for 24 h, indicating that the single fcc CoCrFeNi HEA solid solution forms in MA process. In order to verify the mixing homogeneity of each metal element, CoCrFeNi HEA powder prepared by MA was investigated by EDS and SEM at secondary electron (SE) and back-scattered electron (BSE) modes, as shown in Fig. 3. It can be seen that the CoCrFeNi HEA powder particles are non-spherical and irregularly-shaped, and their average particle size is about 80 μm. In addition, the as-milled CoCrFeNi HEA powder possesses rough surface due to the long-term intense collision between particles and grinding ball, which results in repeated cold welding and fracture of powders. According to Fig.3c and 3d, the four metal elements of CoCrFeNi HEA are distributed uniformly, and their contents are shown in Table 1.

Fig.4 presents SEM-BSE images and corresponding EDS element distributions of bulk CoCrFeNi HEA prepared by MA-VHPS. It can be seen from Fig.4a that the dark phases are dispersed in the matrix, which indicates the segregation and aggregation of some elements or phases. Moreover, the size of the dark phases with irregular shape is less than 4 μm. The black dots are pits on the surface of bulk CoCrFeNi HEA. According to Fig. 4c, the Co, Fe, and Ni elements are dispersed uniformly in the matrix. However, the Cr element is segregated from the CoCrFeNi HEA matrix, because the hardness of Cr is higher than that of the other three metals. Therefore, the repeated cold welding has slight influence on Cr and the fracture between particles hardly occurs on Cr particles during the MA process, resulting in slower atomic diffusion rate of Cr element. Thus, prolonging the duration of

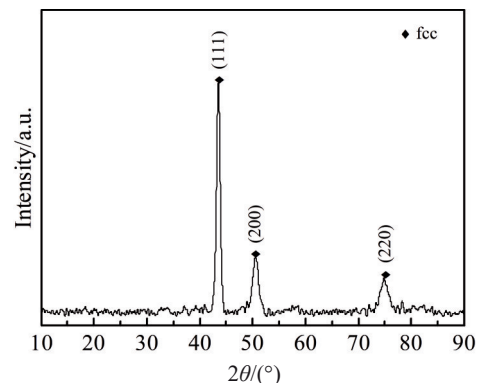


Fig.2 XRD pattern of CoCrFeNi HEA powder prepared by MA

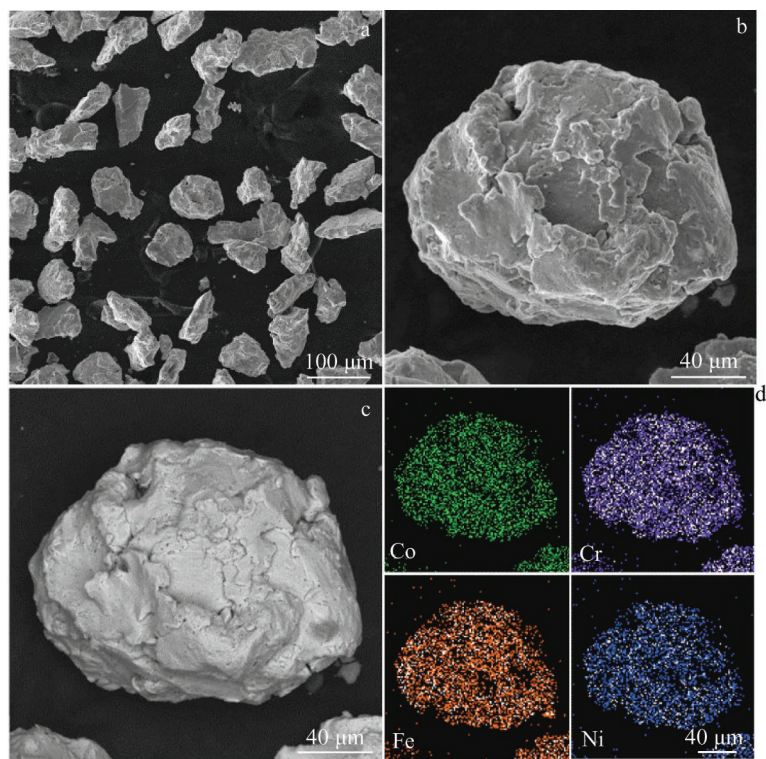


Fig.3 SEM images of CoCrFeNi HEA powder prepared by MA at SE (a, b) and BSE (c) modes; EDS element distributions in CoCrFeNi HEA powder prepared by MA (d)

Table 1 Composition of as-milled CoCrFeNi HEA powders prepared by MA (at%)			
Co	Cr	Fe	Ni
25	25	26	24

ball milling and heat treatment can better homogenize the Cr element distribution in the matrix.

OM image of the bulk CoCrFeNi HEA is shown in Fig.5. It can be seen that the bulk CoCrFeNi HEA has a small grain size of <50 μm, which is ascribed to the fact that the low processing temperature can effectively prevent the grain growth, therefore significantly improving the mechanical properties of the bulk CoCrFeNi HEA due to the fine grain strengthening effect.

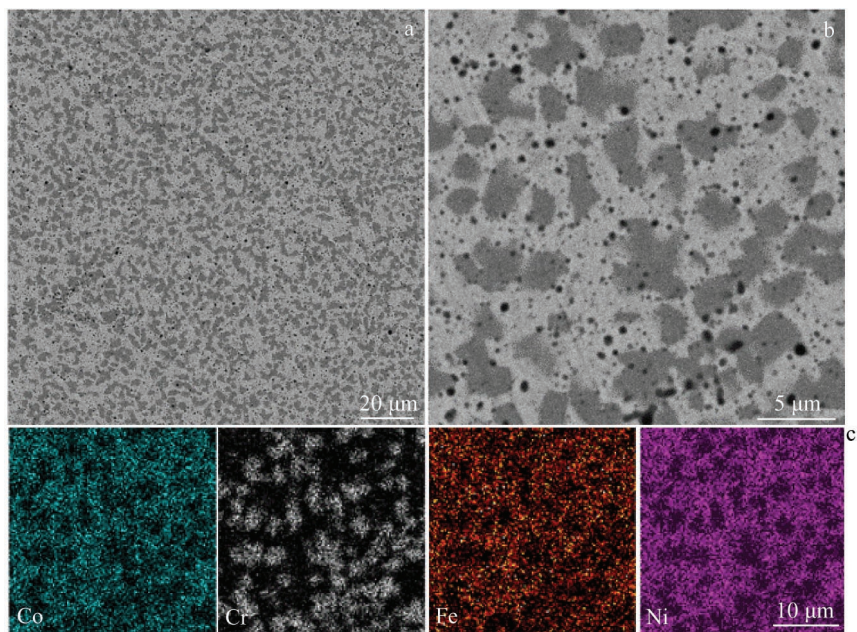


Fig.4 SEM-BSE images (a, b) and corresponding EDS element distributions of bulk CoCrFeNi HEA prepared by MA-VHPS



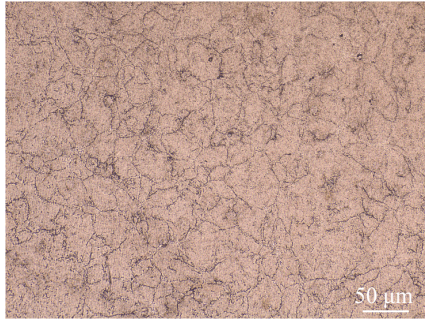


Fig.5 OM image of bulk CoCrFeNi HEA prepared by MA-VHPS

## 2.2 Mechanical properties

Fig.6 presents the engineering stress-strain curves of bulk CoCrFeNi HEA prepared by MA-VHPS, FFC-VHPS, and arc-melting methods. The ultimate tensile strength (UTS) of CoCrFeNi HEA prepared by MA-VHPS, FFC-VHPS, and arc-melting methods is 721, 661, and 522 MPa, respectively. CoCrFeNi HEA prepared by MA-VHPS has the best elongation, compared with that prepared by FFC-VHPS and arc-melting methods. The excellent UTS of CoCrFeNi HEA prepared by MA-VHPS process is mainly attributed to the fine grain strengthening effect. Meanwhile, the uniform distribution of elements also ensures the excellent ductility of CoCrFeNi HEA. UTS of CoCrFeNi HEA prepared by FFC-VHPS is between that prepared by MA-VHPS and arc-melting method, but its plasticity is the lowest among these three HEAs. There are two main reasons for these results. Firstly, UTS can be improved by the secondary phase  $\text{Cr}_7\text{C}_3$

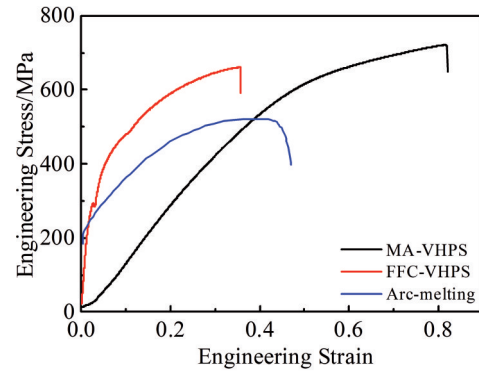


Fig.6 Stress-strain curves of CoCrFeNi HEAs prepared by MA-VHPS, FFC-VHPS, and arc-melting methods

and fine grain strengthening effect, and the cathode carbon deposition accounts for the formation of  $\text{Cr}_7\text{C}_3$  in CoCrFeNi HEA prepared by FFC-VHPS process<sup>[21]</sup>. Secondly, the strength and plasticity of the alloys are decreased by the secondary phase  $\text{Cr}_7\text{C}_3$  and a trace amount of oxygen in CoCrFeNi HEA, which is derived from the incompletely electro-deoxidized oxides in FFC process.

Fig. 7 presents the fracture surfaces of CoCrFeNi HEA prepared by MA-VHPS and FFC-VHPS. The ductile dimples with uniform morphology and size are formed in CoCrFeNi HEA (Fig. 7b), which is the characteristic of plastic fracture. The ductile dimples can also be observed in the fracture surface of CoCrFeNi HEA prepared by FFC-VHPS process (Fig. 7d), but the dimples have irregular morphology and different sizes. The cleavage fracture morphology of river

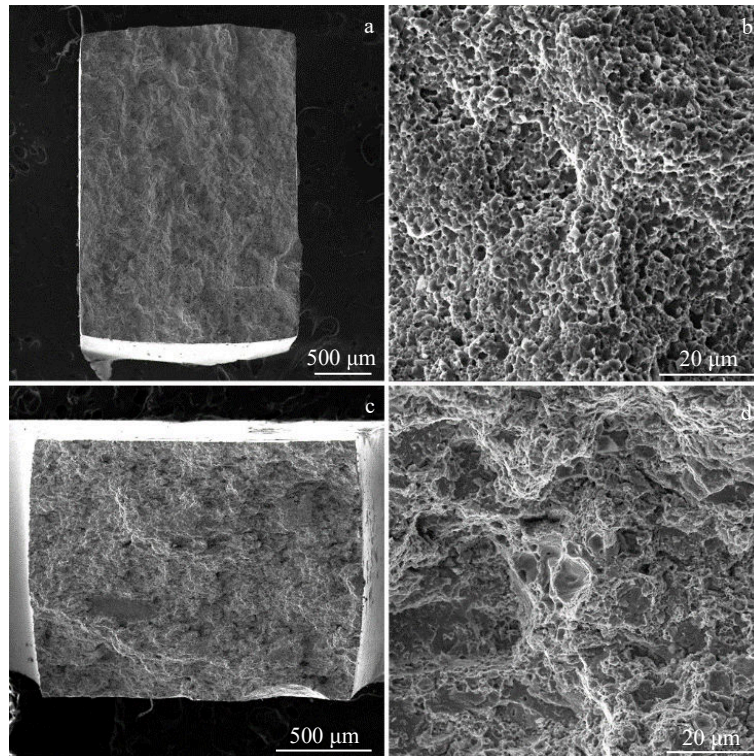


Fig.7 Fracture surfaces of CoCrFeNi HEAs prepared by MA-VHPS (a, b) and FFC-VHPS (c, d) processes

pattern and cracks can be observed in the fracture surface, because of the secondary phase  $\text{Cr}_7\text{C}_3$  and a trace amount of the remaining oxygen. Therefore, the strength and plasticity of CoCrFeNi HEA prepared by FFC-VHPS are lower than those prepared by MA-VHPS process.

Fig.8 displays the hardness of CoCrFeNi HEAs prepared by MA-VHPS, FFC-VHPS, and arc-melting methods. The results show that the hardness of CoCrFeNi HEAs prepared by MA-VHPS (2298.88 MPa) and FFC-VHPS (2403.35 MPa) is about twice larger than that prepared by arc-melting method (1134.84 MPa). The excellent hardness of CoCrFeNi HEAs prepared by MA-VHPS and FFC-VHPS is mainly attributed to the fine grain strengthening effect. The hardness of CoCrFeNi HEA prepared by FFC-VHPS is optimal because of the reinforcement effect of the secondary phase  $\text{Cr}_7\text{C}_3$ .

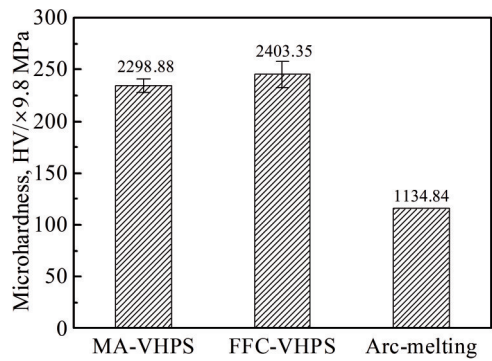


Fig.8 Hardness of CoCrFeNi HEA fabricated by MA-VHPS, FFC-VHPS, and arc-melting methods

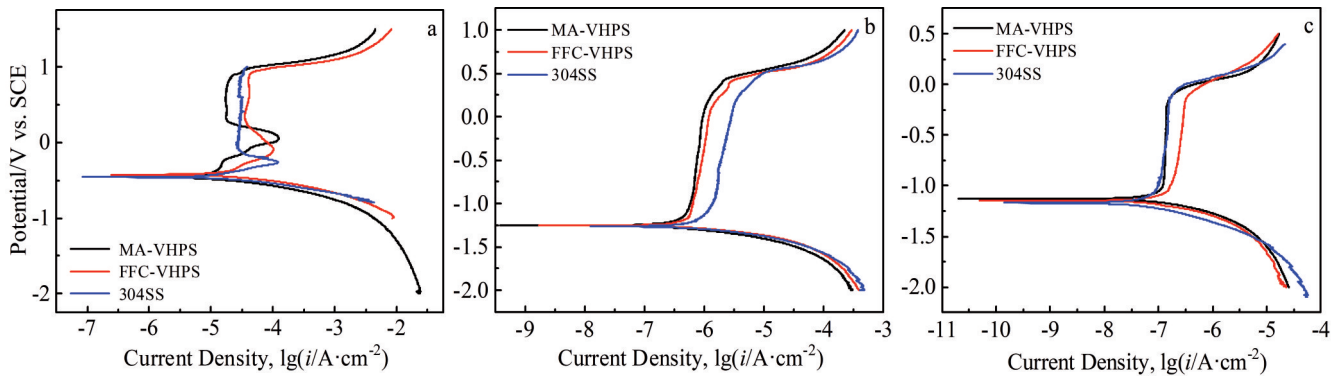


Fig.9 Potentiodynamic polarization curves of 304SS and CoCrFeNi HEAs prepared by MA-VHPS and FFC-VHPS at steady-state in 0.5 mol/L  $\text{H}_2\text{SO}_4$  (a), 1 mol/L KOH (b), and 3.5wt% NaCl (c) solutions

2.3 Potentiodynamic polarization

The potentiodynamic polarization tests of CoCrFeNi HEAs prepared by MA-VHPS and FFC-VHPS and 304SS were conducted in 0.5 mol/L  $\text{H}_2\text{SO}_4$ , 1 mol/L KOH, and 3.5wt% NaCl aqueous solutions, and the results are shown in Fig.9. Fig.9a displays the passive region in the range of  $-0.25\sim1.1$  V vs. SCE<sup>[22]</sup>, because the passivated oxide film is further oxidized or hydroxylated, changing the valence state of  $\text{Cr}^{[23]}$ . According to Table 2, the corrosion potential ( $E_{\text{corr}}$ ) of 304SS and CoCrFeNi HEAs prepared by MA-VHPS and FFC-VHPS methods has slight difference, but the results of corrosion current density ( $i_{\text{corr}}$ ) suggest that the corrosion resistance behavior of CoCrFeNi HEA prepared by MA-VHPS is better than that of HEA prepared by FFC-VHPS and 304SS. Compared with HEA prepared by arc-melting, CoCrFeNi HEA prepared by MA-VHPS has smaller  $E_{\text{corr}}$ . Although  $i_{\text{corr}}$  of CoCrFeNi HEA prepared by MA-VHPS is smaller than that prepared by arc-melting method, the corrosion resistance of these two HEAs is very similar<sup>[24]</sup>.

The obviously passive region can be observed in Fig. 9b, indicating that the stable oxide films are formed. When the applied potential increases to about 0.5 V vs. SCE, the passivation film is broken and the current density increases sharply. According to Table 3, there is no significant difference in  $E_{\text{corr}}$  between 304SS and CoCrFeNi HEAs

prepared by MA-VHPS and FFC-VHPS methods. The  $i_{\text{corr}}$  results indicate that CoCrFeNi HEA prepared by MA-VHPS has better corrosion resistance behavior than that prepared by FFC-VHPS and 304SS do.

Fig.9c shows the direct transition from the Tafel region into the stable passive region, which indicates that the stable oxide films are formed spontaneously at the corrosion potential. The low ion transport rate of the oxide film through the passivated

Table 2 Corrosion potential  $E_{\text{corr}}$  and corrosion current density  $i_{\text{corr}}$  of 304SS and CoCrFeNi HEAs in 0.5 mol/L  $\text{H}_2\text{SO}_4$

Preparation method	$E_{\text{corr}}/\text{V vs. SCE}$	$i_{\text{corr}}/\times 10^{-5} \text{ A}\cdot\text{cm}^{-2}$	Ref.
MA-VHPS	-0.457	1.84	-
FFC-VHPS	-0.425	4.26	[18]
Arc-melting	-0.081	1.67	[20]
304SS	-0.351	5.12	-

Table 3 Corrosion potential  $E_{\text{corr}}$  and corrosion current density  $i_{\text{corr}}$  of 304SS and CoCrFeNi HEAs in 1 mol/L KOH

Preparation method	$E_{\text{corr}}/\text{V vs. SCE}$	$i_{\text{corr}}/\times 10^{-7} \text{ A}\cdot\text{cm}^{-2}$	Ref.
MA-VHPS	-1.254	1.34	-
FFC-VHPS	-1.251	2.06	[18]
304SS	-1.279	3.01	-

**Table 4** Corrosion potential  $E_{\text{corr}}$  and corrosion current density  $i_{\text{corr}}$  of 304SS and CoCrFeNi HEAs in 3.5wt% NaCl solution

Preparation method	$E_{\text{corr}}/\text{V vs. SCE}$	$i_{\text{corr}}/\times 10^{-8} \text{ A}\cdot\text{cm}^{-2}$	Ref.
MA-VHPS	-1.130	2.29	-
FFC-VHPS	-1.147	2.45	[18]
Arc-melting	-0.260	3.15	[23]
304SS	-1.169	2.28	-

region represents the excellent corrosion resistance<sup>[25-27]</sup>. According to Table 4, the  $E_{\text{corr}}$  of CoCrFeNi HEA prepared by arc-melting<sup>[22]</sup> is smaller than that of HEAs prepared by MA-VHPS and FFC-VHPS methods and 304SS in 3.5wt% NaCl solution. The low  $i_{\text{corr}}$  results show that the 304SS and CoCrFeNi HEAs prepared by different methods have excellent corrosion resistance in 3.5wt% NaCl aqueous solution<sup>[28]</sup>.

### 3 Conclusions

1) CoCrFeNi high-entropy alloy (HEA) with single phase face-centered cubic structure prepared by mechanical alloying (MA) and vacuum hot pressing sintering (VHPS) has uniform element distribution and homogeneous structure.

2) The high hardness of Cr element leads to slight segregation from the HEA matrix. The low processing temperature of VHPS can effectively prevent the grain growth, resulting in the fact that the grain size of CoCrFeNi HEA is generally less than 50  $\mu\text{m}$ .

3) The CoCrFeNi HEA prepared by MA-VHPS exhibits excellent ultimate tensile strength (721 MPa), because of the fine grain strengthening effect. The hardness of CoCrFeNi HEA prepared by MA-VHPS (2298.88 MPa) is about twice larger than that prepared by the traditional arc-melting method. The corrosion resistance of CoCrFeNi HEA prepared by MA-VHPS is also comparable to that of 304SS and HEAs prepared by electrochemical reduction-VHPS and arc-melting method in different solutions.

4) CoCrFeNi HEA prepared by MA-VHPS exhibits an excellent combination of strength and plasticity, a relatively good hardness, and a comparable corrosion resistance performance, revealing the application potential of MA-VHPS process.

### References

- Cantor B, Chang I T H, Knight P et al. *Mater Sci Eng A*[J], 2004, 375-377: 213
- Yeh J W, Chen S K, Lin S J et al. *Adv Eng Mater*[J], 2004, 6(5): 299
- Zhang Y, Zuo T T, Tang Z et al. *Prog Mater Sci*[J], 2014, 61: 1
- Zhang W R, Liaw P K, Zhang Y. *Sci China Mater*[J], 2018, 61: 2
- Chang H T, Huo X F, Li W P et al. *Rare Metal Mat Eng*[J], 2020, 49(10): 3633
- Li Yanchao, Li Laiping, Gao Xuanqiao et al. *Rare Metal Mat Eng*[J], 2020, 49(12): 4365 (in Chinese)
- Wang W R, Wang W L, Wang S C et al. *Intermetallics*[J], 2012, 26: 44
- Wang W R, Wang W L, Yeh J W. *J Alloy Compd*[J], 2014, 589: 143
- Kao Y F, Chen T J, Chen S K et al. *J Alloy Compd*[J], 2009, 488(1): 57
- Li R D, Niu P D, Yuan T C et al. *J Alloy Compd*[J], 2018, 746: 125
- Luo S C, Gao P, Yu H C et al. *J Alloy Compd*[J], 2019, 771: 387
- Ma S G, Zhang S F, Gao M C et al. *JOM*[J], 2013, 65(12): 1751
- Ma S G, Zhang S F, Qiao J W et al. *Intermetallics*[J], 2014, 54: 104
- Varalakshmi S, Kamaraj M, Murty B S. *J Alloy Compd*[J], 2008, 460(1-2): 253
- Kilmametov A, Kulagin R, Mazilkin A et al. *Ser Mater*[J], 2019, 158: 29
- Varalakshmi S, Kamaraj M, Murty B S. *Mat Sci Eng A*[J], 2010, 527(4-5): 1027
- Ge W J, Wu B, Wang S R et al. *Adv Powder Technol*[J], 2017, 28(10): 2556
- Xie Y C, Cheng H, Tang Q H et al. *Intermetallics*[J], 2018, 93: 228
- Joo S H, Kato H, Jang M J et al. *Mat Sci Eng A*[J], 2017, 689: 122
- Yang Y, Luo X Y, Ma T X et al. *J Alloy Compd*[J], 2021, 864: 158 717
- Wang B, Huang J, Fan J H et al. *J Electrochem Soc*[J], 2017, 164(14): E575
- Kao Y F, Lee T D, Chen S K et al. *Corr Sci*[J], 2010, 52(3): 1026
- Chen Y Y, Chou L B, Shih H C. *Mater Sci Eng A*[J], 2005, 396(1-2): 129
- Shi Y Z, Yang B, Liaw P K. *Metals*[J], 2017, 7(2): 43
- Hsu Y J, Chiang W C, Wu J K. *Mater Chem Phys*[J], 2005, 92(1): 112
- Shi Y Z, Mo J K, Zhang F Y et al. *J Alloys Compd*[J], 2020, 844: 156 014
- Shi Y Z, Liam C, Rui F et al. *Corr Sci*[J], 2018, 133: 120
- Shi Y Z, Yang B, Xie X et al. *Corr Sci*[J], 2017, 119: 33

## 机械合金化联合真空热压烧结工艺制备 CoCrFeNi 高熵合金的力学性能和耐腐蚀性能

杨 宇<sup>1,2</sup>, 陈俊宇<sup>1,2</sup>, 马通祥<sup>1,2</sup>, 扈玫珑<sup>1,2</sup>

(1. 重庆大学 材料科学与工程学院, 重庆 400044)

(2. 重庆大学 钒钛冶金及新材料重庆市重点实验室, 重庆 400044)

**摘 要:** 采用机械合金化和真空热压烧结工艺制备了 CoCrFeNi 高熵合金。采用 X 射线衍射仪、扫描电子显微镜、电感耦合等离子体发射光谱和光学显微镜对产物的相结构和微观结构进行了表征, 并采用万能试验机、维氏硬度计和电化学工作站对其力学性能和耐腐蚀性能进行了研究。结果表明: 与电化学还原联合热压烧结工艺以及电弧熔炼法制备的 CoCrFeNi 高熵合金性能相比, 机械合金化联合真空热压烧结工艺制备的 CoCrFeNi 高熵合金具有良好的抗拉伸强度和断裂伸长率, 其合金硬度是电弧熔炼法制备合金的 2 倍, 在 0.5 mol/L  $\text{H}_2\text{SO}_4$ 、1 mol/L KOH 和 3.5% (质量分数) NaCl 水溶液中, 该合金具有与 304 不锈钢及电化学还原联合热压烧结工艺或电弧熔炼法制备合金相当的耐腐蚀性能。

**关键词:** 熵值合金; 机械合金化; 真空热压烧结; 力学性能; 耐腐蚀性能

---

作者简介: 杨 宇, 男, 1992 年生, 博士生, 重庆大学材料科学与工程学院, 重庆 400044, E-mail: 20180901053@cqu.edu.cn